

doi:10.3799/dqkx.2017.530

广西东平富 Ga 含锰岩系碳、氧同位素特征及意义

李启来¹, 伊海生^{1,2*}, 夏国清¹, 季长军³, 金峰¹

1. 成都理工大学沉积地质研究院, 四川成都 610059

2. 成都理工大学油气藏地质及开发工程国家重点实验室, 四川成都 610059

3. 中国地质科学院, 北京 100037

摘要:在广西东平碳酸锰矿含锰岩系中发现 Ga 含量高异常, Ga 含量为 $5.16 \times 10^{-6} \sim 82.80 \times 10^{-6}$, 平均含量为 33.76×10^{-6} , 达到了 Ga 矿资源工业品位标准要求, 但目前还未见有产 Ga 锰矿床的报道。为了提升对此富 Ga 现象的认识, 对其进行了碳、氧同位素特征研究。结果显示: 矿石和围岩 $\delta^{13}C_{PDB}$ 值分别为 $-6.40\% \sim -2.20\%$ 、 $-8.90\% \sim 0.90\%$, $\delta^{18}O_{PDB}$ 值分别为 $-9.00\% \sim -7.90\%$ 、 $-9.90\% \sim -3.90\%$ 。研究表明: (1) 有机质参与了碳酸锰矿形成; (2) 含锰岩系为热水沉积成因, Ga 来源与海底热液活动密切相关; (3) 海底热液活动一方面为形成锰碳酸盐直接或间接提供了大量有机质, 另一方面为形成富 Ga 含锰岩系带来了大量 Ga, 被锰的氧化物或氢氧化物、海洋生物(多为热液微生物)所吸附、富集, 经复杂的成岩、成矿作用而最终赋存于含锰岩系之中形成富 Ga 含锰岩系。

关键词: 锰矿床; Ga 异常; 碳、氧同位素; 矿床。

中图分类号: P618.74

文章编号: 1000-2383(2017)09-1508-11

收稿日期: 2016-11-27

Characteristics and Implication of Carbon and Oxygen Isotopes in Ga-Rich Manganese-Bearing Rock Series in Dongping, Guangxi

Li Qilai¹, Yi Haisheng^{1,2*}, Xia Guoqing¹, Ji Changjun³, Jin Feng¹

1. Institute of Sedimentary Geology, Chengdu University of Technology, Chengdu 610059, China

2. State Key Laboratory of Oil and Gas Reservoir Geology and Exploration, Chengdu University of Technology, Chengdu 610059, China

3. Chinese Academy of Geological Sciences, Beijing 100037, China

Abstract: Recently, an unusually high content of Ga was discovered in manganese carbonate deposits of the Beisi Formation in Dongping area, Guangxi. The content of Ga is between 5.16×10^{-6} and 82.80×10^{-6} , and the average content is 33.76×10^{-6} , which reaches the industrial grade of Ga. But, to date Ga is not extracted from manganese deposits. In order to deepen the understanding of this phenomenon, the results of carbon and oxygen isotopes in the Ga-rich manganese-bearing rock series are reported in this paper. The results show that $\delta^{13}C_{PDB}$ of ores and host rocks are -6.40% to -2.20% and -8.90% to 0.90% , respectively; $\delta^{18}O_{PDB}$ of ores and host rocks are -9.00% to -7.90% and -9.90% to -3.90% , respectively. The results of the research show that (1) organic matter participates in the formation of manganese carbonate; (2) the Ga-rich manganese-bearing rock series belong to hydrothermal sedimentary genesis, and the source of Ga is related to seafloor hydrothermal activity; (3) seafloor hydrothermal activity plays a key role in the mineralization process of this Ga-rich manganese-bearing rock series, it directly or indirectly provides a large amount of organic matter to formation of manganese carbonates, on the other hand, it brought a lot of Ga that can be adsorbed by manganese oxides or hydroxide, marine organisms (mostly hydrothermal microorganism), then Ga concentrated in manganese-bearing rock series by complex diagenesis and mineralization.

Key words: manganese deposit; Ga anomaly; carbon and oxygen isotopes; ore deposits.

基金项目: 国家科技支撑计划专项项目(No.2011BAB04B10-2).

作者简介: 李启来(1989-), 男, 博士研究生, 主要从事沉积地球化学研究. ORCID: 0000-0002-7449-9946. E-mail: zg0605@126.com

* **通讯作者:** 伊海生, ORCID: 0000-0002-6679-681X. E-mail: yhs@cdu.edu.cn

引用格式: 李启来, 伊海生, 夏国清, 等, 2017. 广西东平富 Ga 含锰岩系碳、氧同位素特征及意义. 地球科学, 42(9): 1508-1518.

Ga 是一种在民用和军事方面均得到广泛应用的战略金属,是电子工业不可缺少的关键性材料(Moskalyk,2003),主要产于铝土矿、闪锌矿及煤矿之中,尚未见有产 Ga 锰矿床的报道(Telford,2001;Dai *et al.*,2012;Sverdrup and Ragnarsdóttir,2014).通常,沉积岩中 Ga 含量低于其克拉克值 19.00×10^{-6} (Dubinin *et al.*,2008);现代大洋热水铁锰沉积中 Ga 平均含量仅为 11.70×10^{-6} (Baturin *et al.*,2014);碳酸盐岩中 Ga 平均含量为 4.00×10^{-6} (陈骏和王鹤年,2004).但是,Ga 在古代和现代铁锰沉积中也能够富集.例如,印度奥利萨邦 Purnapani 锰矿层中 Ga 平均含量为 24.68×10^{-6} (Mishra *et al.*,2006),日本海梅德韦杰夫海底山铁锰沉积中 Ga 含量高达 874.00×10^{-6} (Mikhailik and Khanchuk,2011).最近,在“十二五”国家科技支撑计划项目执行期间,笔者发现广西东平碳酸锰矿含锰岩系存在 Ga 含量高异常,其含量为 $5.16 \times 10^{-6} \sim 82.80 \times 10^{-6}$,平均含量为 33.76×10^{-6} ,达到了 Ga 的工业品位最低要求(邵厥年和陶维屏,2010).

然而,古代和现代铁锰沉积富 Ga 现象还未引起足够的注意.在古代含锰岩系研究中涉及 Ga 含量的报道仅限于实验数据介绍(Sugisaki *et al.*,1991;Mishra *et al.*,2006;Kazachenko *et al.*,2006;杨瑞东等,2009,2010;何志威等,2013,刘志臣等 2013;张超,

2013),却未对现象出现的原因、过程等进行分析 and 讨论;在现代大洋铁锰沉积研究中涉及 Ga 含量的文献多属现象报道 (Anikeeva *et al.*,2008;Dubinin *et al.*,2008;Mikhailik *et al.*,2009;Baturin *et al.*,2010,2012;Mikhailik and Khanchuk,2011),部分学者对 Ga 的物质来源 (Dubinin and Uspenskaya,2006;Mikhailik *et al.*,2015)和赋存形式(Koschinsky and Hein,2003;Mikhailik *et al.*,2015)等进行了初步研究.但是,目前还未见有针对富 Ga 含锰岩系碳、氧同位素特征 的报道和研究.

另外,东平富 Ga 含锰岩系实际上是东平氧化锰矿的矿胚层,一直未受到关注,目前已有研究成果主要集中在氧化锰矿层(祝寿泉,1997;李升福等,2009).

鉴于此,本文通过碳、氧同位素特征研究,分析了碳同位素来源、成矿温度和古盐度以及碳、氧同位素相关关系,讨论了 Ga 的物质来源,以期 为研究富 Ga 含锰岩系提供新资料,为研究东平锰矿提供新信息.

1 地质背景和矿床地质

1.1 地质背景

研究区地处桂西南锰矿区东南部(图 1),构造上

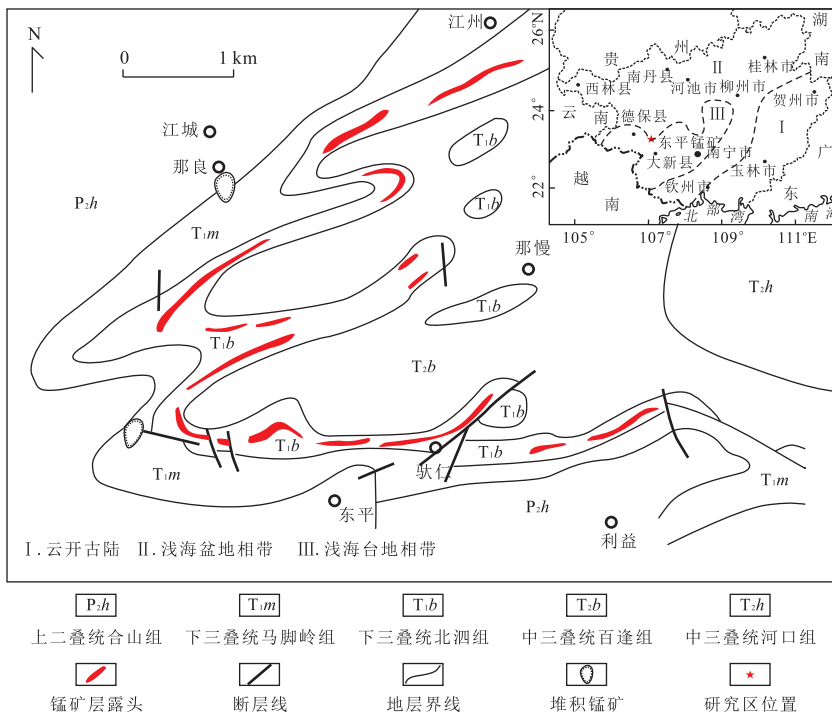


图 1 东平锰矿区地质简图

Fig.1 Geological sketch of Dongping manganese orefield

据茹廷锵(1992)

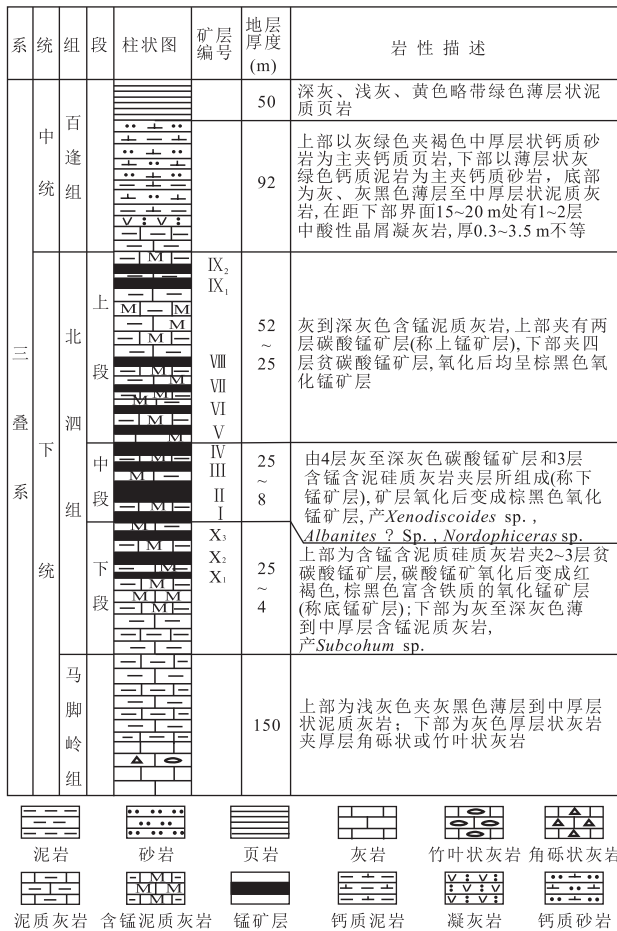


图 2 东平锰矿区综合地层柱状图

Fig.2 Comprehensive stratigraphic column of Manganese-bearing rock assemblages in Dongping area

据刘腾飞(1996)

位于右江裂陷盆地西南缘地州至向都弧形褶皱带下雷—灵马坳陷的西南端,为一轴向北东—南西的复式向斜构造(图 1)。二叠纪末,桂西地区进入裂谷坳陷期;早三叠世,裂陷带快速扩张,碳酸盐台地发生裂解破碎,形成了大面积的坳陷区,产生了以深水、半深水的台盆、台沟与浅水的条带状碳酸盐台地相间的古地理格局;中三叠世,火山活动活跃,东平地区百逢组底部发育有 1~2 层凝灰岩;晚期印支运动造成洋盆关闭,结束了本地区海相沉积的历史(刘腾飞,1996)。

区内出露地层有上二叠统合山组(P_2h)、下三叠统马脚岭组(T_1m)、北泗组(T_1b)、中三叠统百逢组(T_2b)、河口组(T_2h)。富锰层位为北泗组,主要由泥灰岩、硅质灰岩、泥质硅质灰岩及含锰灰岩等一套岩石组成。早三叠世晚期,在金沙江—古特提斯洋盆向华南板块西缘消减俯冲加强及热扩散后的收缩作用和滨太平洋构造挤压作用下形成的断裂坳陷,控制着该时期锰矿的形成与分布。锰矿产于浅海盆地

边缘坳陷相带,夹于含硅质的泥灰岩中(刘腾飞,1996;李升福等,2009),矿层沿向斜两翼依次出现。

1.2 矿床地质

东平锰矿共有 13 个锰矿层,分布于北泗组下、中、上三段(图 2)。下段分布有 X_1 、 X_2 、 X_3 三个矿层,为灰色、灰黑色厚至薄层状含锰泥质硅质灰岩、泥灰岩,厚 4~25 m;中段分布有 I、II、III、IV 四个矿层,由 4 层灰至深灰色碳酸锰矿层和 3 层含锰泥质硅质灰岩夹层组成,厚 8~25 m;上段分布有 IX₁、IX₂ 及 V、VI、VII、VIII 六个矿层,为灰至深灰色含锰泥质灰岩及泥质页岩,厚 25~52 m。原生矿石(碳酸锰矿)为深灰色、灰黑色含锰灰岩,主要由锰方解石、含锰方解石、方解石、石英、绢云母和绿泥石组成,含有少量黄铁矿、黄铜矿、闪锌矿、赤铁矿及白云石等,偶见有楣石、金红石、锆石、磷灰石、电气石、白钛石、磁铁矿、钛铁矿等(祝寿泉,2001)。笔者通过碳酸锰矿成分分析,结果显示其 Mn 含量为 3.79%~11.80%, Fe 含量为 2.57%~28.09%, P 含量为 0.10%~3.89%, Si 含量为 23.42%~35.89%, CaO 含量为 7.32%~15.23%, MgO 含量为 3.67%~4.46%, Mn/Fe 值为 0.14~4.19, P/Fe 值为 0.01~0.13。同时,其 Ga 含量异常高,为 15.80×10^{-6} ~ 70.90×10^{-6} , 平均含量为 44.09×10^{-6} 。碳酸锰矿具有“高 Si、高 P、高 Fe、贫 Mn、富 Ga”的特点。

东平富 Ga 含锰岩系主要由碳酸锰矿、含锰硅质泥灰岩、硅质泥灰岩,及少量含炭硅质泥灰岩和硅质泥岩组成,具有热水沉积特征的纹层状构造(图 3a)、条带状构造(图 3b)、斑状结构(图 3c)和角砾状构造(图 3d),与海底热水喷流沉积形成的贵州镇宁泥盆系大型重晶石矿床相似(高军波等,2013)。此外,还含有鲕豆粒结构,在后期石英脉中常见有黄铁矿。

2 测试方法及结果

共有 18 件样品采自东平地区地表和锰矿钻探浅井,采集层位为下三叠统北泗组,其中矿石样品 11 件,围岩样品 7 件,样品具体分布见表 1。对样品进行了碳、氧同位素分析,由核工业北京地质研究院完成。分析仪器采用的是德国 Thermo Scientific 公司生产的 MAT 253 稳定同位素质谱仪, $\delta^{18}O$ 和 $\delta^{13}C$ 均以 PDB 为标准,分析精度为 $\pm 0.20\%$, 样品的具体制备方法和分析流程详见相关文献(Ghosh *et al.*, 2006; 韩晓涛等, 2016), 结果见表 1。

由于 $\delta^{18}O$ 受成岩蚀变的影响远大于 $\delta^{13}C$, 故

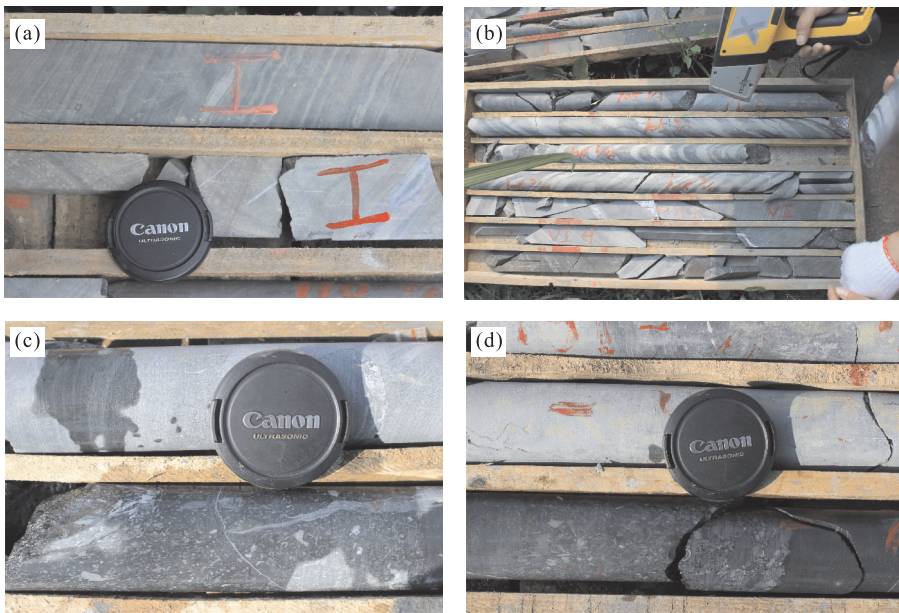


图 3 东平富 Ga 含锰岩系沉积结构和构造

Fig.3 Textures and sedimentary structures of Dongping Ga-rich manganese-bearing rock series

a. 纹层状构造; b. 条带状构造; c. 斑状结构; d. 角砾状构造

表 1 东平富 Ga 含锰岩系碳、氧同位素组成及古温度和 Z 值

Table 1 $\delta^{13}\text{C}_{\text{PDB}}$, $\delta^{18}\text{O}_{\text{PDB}}$, Z values and paleotemperatures of Dongping Ga-rich manganese-bearing rock series

序号	样品编号	采样深度(m)	岩石类型	$\delta^{13}\text{C}_{\text{PDB}}(\text{‰})$	$\delta^{18}\text{O}_{\text{PDB}}(\text{‰})$	$t_1(\text{°C})$	$t_2(\text{°C})$	$t_3(\text{°C})$	Z
1	TK-14	地表	硅质泥灰岩	0.90	-3.90	35.90	33.53	35.50	127.20
2	7213-H05	138	硅质泥灰岩	-2.20	-9.60	66.74	70.58	68.16	118.01
3	7213-H07	177	碳酸锰矿	-6.40	-8.20	59.16	60.68	59.54	110.11
4	7213-H08	184	硅质泥灰岩	-2.90	-9.60	66.74	70.58	68.16	116.58
5	7213-H10	190	硅质泥灰岩	-2.90	-9.30	65.11	68.41	66.28	116.73
6	7213-H11	192	碳酸锰矿	-3.50	-9.00	63.49	66.27	64.42	115.65
7	7213-H12	196	硅质泥灰岩	-2.70	-9.90	68.36	72.78	70.06	116.84
8	7601-H07	151	硅质泥灰岩	-2.40	-9.30	65.11	68.41	66.28	117.75
9	7601-H08	154	碳酸锰矿	-3.50	-8.90	62.95	65.56	63.80	115.70
10	7601-H11	159	碳酸锰矿	-4.80	-8.70	61.87	64.15	62.58	113.14
11	7601-H16	251	碳酸锰矿	-4.10	-8.40	60.24	62.06	60.75	114.72
12	7601-H18	260	碳酸锰矿	-3.50	-8.90	62.95	65.56	63.80	115.70
13	7601-H20	267	碳酸锰矿	-3.50	-8.60	61.33	63.45	61.96	115.85
14	7601-H22	280	硅质泥灰岩	-2.60	-9.60	66.74	70.58	68.16	117.19
15	1102-H10	128	碳酸锰矿	-2.20	-8.80	62.41	64.85	63.19	118.41
16	1102-H12	131	碳酸锰矿	-2.40	-7.90	57.54	58.63	57.74	118.45
17	KC-1	地表	碳酸锰矿	-5.40	-8.50	60.79	62.75	61.36	112.01
18	KC-2		碳酸锰矿	-5.50	-8.60	61.33	63.45	61.96	111.75

常用 $\delta^{18}\text{O}$ 值来判别岩石样品是否保留了碳、氧同位素原始组成 (Hudson, 1977), 即当 $\delta^{18}\text{O}_{\text{PDB}} > -10.00\text{‰}$ 时, 数据可靠 (Li *et al.*, 2009; 王宏伟等, 2013). 样品 $\delta^{18}\text{O}_{\text{PDB}}$ 值均大于 -10.00‰ . 因此, 测试结果可靠, 基本保留了原始沉积的碳、氧同位素组成特征.

3 碳、氧同位素特征

3.1 碳同位素分析

通常, 海相碳酸盐中的碳有 3 种来源, 即海水、先存碳酸盐矿物的溶解和有机质的降解 (Okita *et al.*, 1988). 其中, 前两种来源的 $\delta^{13}\text{C}_{\text{PDB}}$ 值为 $0 \pm 2\text{‰}$ (Diaz-del-Río *et al.*, 2003), 为无机碳来源; 有机

碳来源的 $\delta^{13}\text{C}_{\text{PDB}}$ 值多为 -20% ~ -30% , 平均值为 -25% (Okita and Shanks, 1992); 混合来源的 $\delta^{13}\text{C}_{\text{PDB}}$ 值则介于无机碳来源和有机碳来源之间 (Coleman *et al.*, 1982).

矿石 $\delta^{13}\text{C}_{\text{PDB}}$ 值为 -6.40% ~ -2.20% , 平均值为 -4.10% , 围岩 $\delta^{13}\text{C}_{\text{PDB}}$ 值集中分布于 -2.90% ~ -2.20% , 平均值为 -2.60% , 还有一件样品 $\delta^{13}\text{C}_{\text{PDB}}$ 值为 0.90% , 两者均显示出混合碳源的特点. 总体上, 矿石 $\delta^{13}\text{C}_{\text{PDB}}$ 值较围岩更为偏负, 说明有机碳源所占比例更大. 另外, 笔者通过有机质含量 (TOC) 分析, 结果显示该套富 Ga 含锰岩系 TOC 较高, 如果按 $\text{TOC} > 0.40\%$ 为标准, 则有 45.00% 的样品可以达到生油岩标准.

3.2 氧同位素及古温度分析

矿石 $\delta^{18}\text{O}_{\text{PDB}}$ 值为 -9.00% ~ -7.90% , 平均值为 -8.60% ; 围岩 $\delta^{18}\text{O}_{\text{PDB}}$ 值集中分布于 -9.90% ~ -9.30% , 平均值为 -9.60% , 仅一件样品 $\delta^{18}\text{O}_{\text{PDB}}$ 值较高, 为 -3.90% .

$\delta^{18}\text{O}$ 值广泛用于推算成岩流体的 $\delta^{18}\text{O}$ 组成及其形成温度. 根据外部测温法原理, 假定水体 $\delta^{18}\text{O}_{\text{SMOW}} = 0.00\%$, 古温度计算公式 (Shackleton and Kennett, 1975): $t_1 = 14.8 - 5.41 \times \delta^{18}\text{O}_{\text{PDB}}$; $t_2 = 1.62 \times 10^4 / (56.75 + \delta^{18}\text{O}_{\text{PDB}}) - 273$; $t_3 = 16.9 - 4.38 \times \delta^{18}\text{O}_{\text{PDB}} + 0.1 \times (\delta^{18}\text{O}_{\text{PDB}})^2$, 据此反演结果列于表 1. 围岩古温度集中分布在 $66.60\sim 70.40\text{ }^\circ\text{C}$, 平均值为 $68.18\text{ }^\circ\text{C}$, 另有一件地表样品古温度为 $34.98\text{ }^\circ\text{C}$; 矿石古温度为 $57.97\sim 64.73\text{ }^\circ\text{C}$, 平均值为 $62.20\text{ }^\circ\text{C}$. 总体上, 矿石和围岩古温度分布集中.

利用矿物与水体的同位素分馏关系也可以推算古温度 (伊海生等, 2014). 假设围岩为纯的方解石 (CaCO_3), 矿石为纯的菱锰矿 (MnCO_3), 且矿物与相应的成岩流体均达到同位素平衡; 设定水溶液 $\delta^{18}\text{O}_{\text{SMOW}}$ 值 (-1.00% ~ 1.00%) 与现代和古海水 (Shackleton and Kennett, 1975) 相当; 方解石与水体的分馏方程: $1000 \ln \alpha_{\text{calcite-water}} = 2.78 \times 10^6 / T^2 - 2.89$ (O'Neil and Epstein, 1966); 菱锰矿与水体的分馏方程: $1000 \ln \alpha_{\text{rhodochrosite-water}} = 4.19 \times 10^6 / T^2 - 4.59 \times 10^3 / T + 1.72$ (Zheng, 1999). 据此推算出围岩古温度集中分布在 $59.00\sim 78.00\text{ }^\circ\text{C}$, 还有一件样品古温度为 $28.00\sim 38.00\text{ }^\circ\text{C}$ (图 4a); 矿石古温度为 $71.00\sim 92.00\text{ }^\circ\text{C}$ (图 4b).

对比来看, 围岩的两种古温度反演结果较为一致, 而矿石的两种古温度反演结果相差较大. 这是由于围岩为硅质泥灰岩, 其主要成分为方解石, 而矿石主要成分为钙菱锰矿和锰方解石 (祝寿泉, 2001), 与纯的菱锰矿在成分上相差较大.

上述两种古温度反演结果均表明含锰岩系为热水沉积成因.

3.3 古盐度分析

$\delta^{18}\text{O}$ 值和 $\delta^{13}\text{C}$ 值随着成岩环境盐度的增加而增大 (Keith and Weber, 1964). 据此, Keith and Weber (1964) 提出综合利用 $\delta^{18}\text{O}$ 值和 $\delta^{13}\text{C}$ 值可计算古盐度 (Z), 其公式为 $Z = 2.048 \times (\delta^{13}\text{C}_{\text{PDB}} + 50) + 0.498 \times (\delta^{18}\text{O}_{\text{PDB}} + 50)$. 当 $Z \geq 120$ 时, 判断为海相碳酸盐; 当 $Z < 120$ 时, 判断为湖相碳酸盐. 然而, 一些湖泊的盐度与海水盐度相当, 甚至高于海水. 例如,

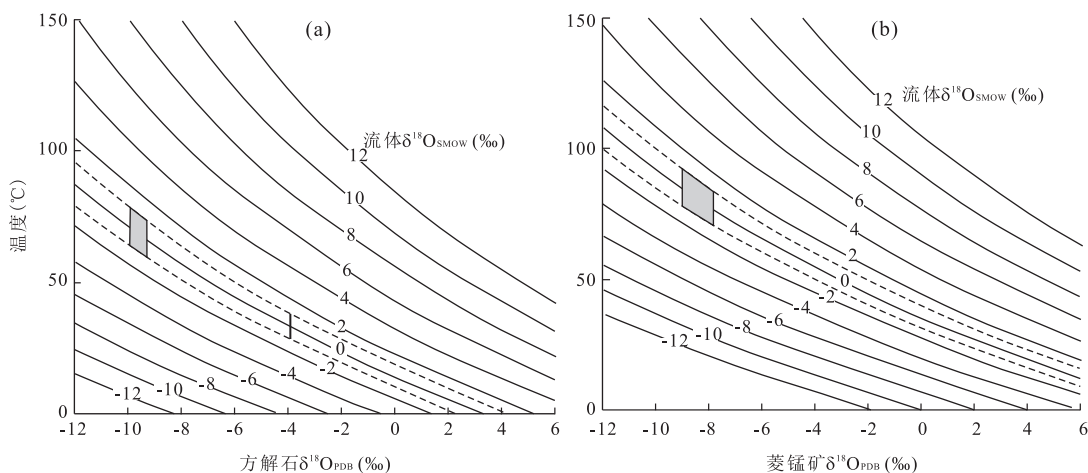


图 4 根据分馏方程计算的不同矿物 (方解石 (a); 菱锰矿 (b)) 温度和流体氧同位素关系

Fig. 4 Plots of equilibrium relationship between temperature and $\delta^{18}\text{O}_{\text{PDB}}$ mineral (calcite (a); rhodochrosite (b)) for various $\delta^{18}\text{O}_{\text{SMOW}}$ fluid from fractionation equation

青藏高原盐湖和青海湖的碳酸盐 Z 值大于 120 (Li *et al.*, 2012). 因此, Z 值不能有效区分海相和湖相碳酸盐沉积, 只能反映成岩流体盐度的相对大小 (Yang *et al.*, 2013).

矿石和围岩 Z 值为 110.11~127.20, 其中仅一件样品 $Z > 120$, 其余 $Z < 120$, 判断为湖相碳酸盐, 而事实上, 东平碳酸锰矿为海相碳酸盐岩. Z 值与 $\delta^{13}\text{C}_{\text{PDB}}$ 值呈极好的相关性 (图 5a), 而与 $\delta^{18}\text{O}_{\text{PDB}}$ 值的相关性一般 (图 5b), 意味着 Z 值主要受 $\delta^{13}\text{C}_{\text{PDB}}$ 的影响 (张振伟等, 2016). 笔者进一步分析发现, $Z \geq 120$ 的样品 $\delta^{13}\text{C}_{\text{PDB}}$ 值为 0.90‰ ; $Z < 120$ 的样品 $\delta^{13}\text{C}_{\text{PDB}}$ 值为 $-6.4\text{‰} \sim -2.2\text{‰}$, 平均值为 -3.56‰ . 因此, 矿石和围岩 Z 值偏低的直接原因是由于其 $\delta^{13}\text{C}_{\text{PDB}}$ 值偏负, 根本原因在于有机质参与了成矿和成岩.

3.4 碳、氧同位素相关性分析

碳、氧同位素的相关关系能够反映海相碳酸盐岩是否遭受成岩蚀变 (Derry, 2010; Macouin *et al.*, 2012). 若 $\delta^{18}\text{O}$ 值与 $\delta^{13}\text{C}$ 值无相关, 则反映出样品未遭受成岩改造, 保留原始同位素组成 (Zuo *et al.*, 2006; Loyd *et al.*, 2015); 若 $\delta^{18}\text{O}$ 值与 $\delta^{13}\text{C}$ 值呈正相关, 则表明样品遭受了成岩改造 (Macouin *et al.*, 2012; Papp *et al.*, 2013; 贾艳艳等, 2015); 若 $\delta^{18}\text{O}$ 值与 $\delta^{13}\text{C}$ 值呈负相关, 在大多数情况下, 反映出样品未遭受成岩蚀变 (Wefer and Berger, 1991; Saalen *et al.*, 1996). 围岩 $\delta^{18}\text{O}_{\text{PDB}}$ 值与 $\delta^{13}\text{C}_{\text{PDB}}$ 值无相关 (图 6a); 矿石 $\delta^{18}\text{O}_{\text{PDB}}$ 值与 $\delta^{13}\text{C}_{\text{PDB}}$ 值呈负相关, 相关系数为 -0.72 (图 6b). 值得注意的是, 矿石 $\delta^{18}\text{O}_{\text{PDB}}$ 值变化范围小, 在 1.10‰ 之内; 而 $\delta^{13}\text{C}_{\text{PDB}}$ 值变化范围大, 在 4.20‰ 之内. 这种变化特征反映出样品 $\delta^{13}\text{C}_{\text{PDB}}$ 值未遭受成岩改造, $\delta^{18}\text{O}_{\text{PDB}}$ 值与原始沉积特征相近 (Fio *et al.*, 2013).

矿石 $\delta^{18}\text{O}_{\text{PDB}}$ 值与 $\delta^{13}\text{C}_{\text{PDB}}$ 值呈负相关, 这一现象在国内外许多碳酸锰矿均有体现 (Okita *et al.*, 1988; Okita and Shanks, 1992; 杨晓飞等, 2013). 这些锰矿的形成多与埋藏有机质氧化过程密不可分 (Kuleshov, 2011); 锰矿的形成还可能与生物甲烷厌氧氧化过程有关, 此过程中, 除了产生 $\delta^{13}\text{C}$ 值极为偏负的甲烷外, 还会形成 $\delta^{13}\text{C}$ 值为正值的碳酸盐胶结物 (Hudson, 1977); 对于 $\delta^{13}\text{C}$ 值十分偏负的锰碳酸盐, 锰矿的形成可能是由海底天然气水合物泄露所导致 (Kuleshov and Brusnitsyn, 2005; 杨克红等, 2016). 后两种成因的锰碳酸盐共同特征是 $\delta^{13}\text{C}$ 值强烈偏负, 例如, 乌拉尔南部 Faizuly 锰矿床 $\delta^{13}\text{C}_{\text{PDB}}$ 值低于 -30.00‰ (Kuleshov and Brusnitsyn, 2005).

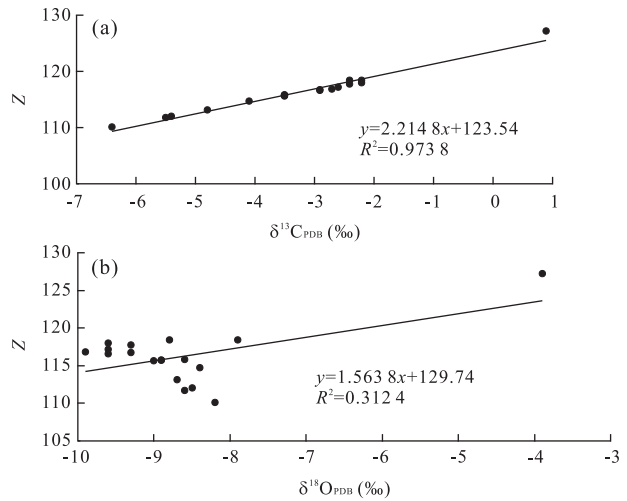


图 5 东平富 Ga 含锰岩系 Z 与 $\delta^{13}\text{C}_{\text{PDB}}$ (a)、 $\delta^{18}\text{O}_{\text{PDB}}$ (b) 的相关关系

Fig.5 Plots of relationship between Z values and $\delta^{13}\text{C}_{\text{PDB}}$ (a) or $\delta^{18}\text{O}_{\text{PDB}}$ (b) for Dongping Ga-rich manganese-bearing rock series

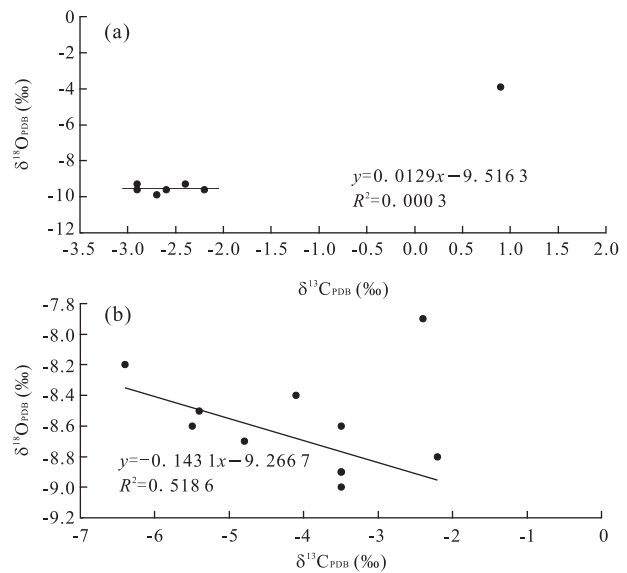


图 6 东平富 Ga 含锰岩系围岩 (a) 和矿石 (b) $\delta^{18}\text{O}_{\text{PDB}}$ 与 $\delta^{13}\text{C}_{\text{PDB}}$ 相关关系

Fig.6 Plots of relationship between $\delta^{13}\text{C}_{\text{PDB}}$ and $\delta^{18}\text{O}_{\text{PDB}}$ for host rocks (a) or ores (b) of Dongping Ga-rich manganese-bearing rock series

矿石 $\delta^{13}\text{C}_{\text{PDB}}$ 最小值为 -6.40‰ , 轻微亏损, 最大值为 -2.20‰ , 也不富集. 因此, 东平碳酸锰矿的形成与甲烷厌氧氧化或海底天然气水合物泄露的关系不大, 而与埋藏有机质降解过程密切相关.

另外, 氧同位素分馏主要受流体温度和盐度的影响, 而在 $\delta^{18}\text{O}$ 值与 $\delta^{13}\text{C}$ 值呈负相关的情况下,

$\delta^{18}\text{O}$ 值主要受控于温度 (Boni *et al.*, 2000; An *et al.*, 2006). 据此, 矿石 $\delta^{18}\text{O}_{\text{PDB}}$ 值与 $\delta^{13}\text{C}_{\text{PDB}}$ 值呈负相关, 直接原因是 $\delta^{18}\text{O}_{\text{PDB}}$ 值受温度降低的影响而增大, 在此过程中, 有机质参与成矿的程度逐渐增加, 使得 $\delta^{13}\text{C}_{\text{PDB}}$ 值越来越偏负.

4 讨论

据前文分析, 东平富 Ga 含锰岩系为热水沉积成因, 有机质参与形成了锰碳酸盐, 该过程主要基于如下反应式: $\text{CH}_2\text{O} + 2\text{MnO}_2 + \text{HCO}_3^- + \text{H}^+ \rightarrow 2\text{MnCO}_3 + 2\text{H}_2\text{O}$ (Okita *et al.*, 1988). 同时, 根据含锰岩系生物标志化合物特征, 参与成矿的有机质多为热液喷口微生物和低等原生藻类, 都直接或间接与海底热液活动相关 (伊帆和伊海生, 2017). 既然如此, 那么含锰岩系中高含量的 Ga 是否也与海底热液活动有关?

海底热液活动产物甚多, 常见有热液流体、热液硫化物、喷口生物等 (曾志刚, 2011). 热液流体富含 Ga, 对此已有诸多报道 (Metz and Trefry, 2000; Baturin *et al.*, 2010, 2011). 同时, 热液硫化物也有富 Ga 的报道 (Iizasa *et al.*, 1999; Noguchi *et al.*, 2007). 例如, 冲绳海槽和菲律宾海 Suiyo 海底山热液硫化物中 Ga 含量分别高达 $3\,700.00 \times 10^{-6}$ 和 $1\,440.00 \times 10^{-6}$ (Noguchi *et al.*, 2007). 因此, 海底热液活动产物能够富 Ga.

现代大洋富 Ga 铁锰沉积研究表明, Ga 的来源可能有 3 个方面, 除了海底热液活动外, 还可能来源于富 Ga 的火山灰 (Mikhailik *et al.*, 2015) 和能够富集 Ga 的海洋生物 (Colwell, 1997; Dubinin and Uspenskaya, 2006). 东平富 Ga 含锰岩系所在层位北泗组凝灰岩中 Ga 平均含量为 16.50×10^{-6} (尹青, 2015), 同正常火成岩均值相当 (刘英俊, 1984), 不具有富 Ga 特点. 因此, Ga 来源与凝灰岩的关系不大, 而与海底热液活动和海洋生物关系密切. 据碳、氧同位素特征研究, 东平富 Ga 含锰岩系为热水沉积成因, 同时生物标志化合物研究显示, 有机质都直接或间接与海底热液活动相关 (伊帆和伊海生, 2017). 故推测 Ga 来源与海底热液活动有关.

进一步推测认为, 海底热液活动在形成富 Ga 碳酸锰矿的过程中起着关键性作用: 它直接或间接提供了形成锰碳酸盐所需的有机质, 同时还带来了大量 Ga, 然后 Ga 被锰的氧化物或氢氧化物所吸附 (Benézéth *et al.*, 1997; Glasby *et al.*, 1997), 还被海

洋生物 (主要是海底热液微生物) 所富集, 而后经复杂的成岩和成矿作用而赋存于含锰岩系之中, 最终形成富 Ga 含锰岩系.

5 结论

(1) 东平富 Ga 含锰岩系矿石和围岩 $\delta^{13}\text{C}_{\text{PDB}}$ 值分别为 $-6.40\% \sim -2.20\%$ 、 $-8.90\% \sim 0.90\%$, $\delta^{18}\text{O}_{\text{PDB}}$ 值分别为 $-9.00\% \sim -7.90\%$ 、 $-9.90\% \sim -3.90\%$. 含锰岩系 $\delta^{13}\text{C}_{\text{PDB}}$ 值低于正常海水, 矿石 $\delta^{18}\text{O}_{\text{PDB}}$ 值与 $\delta^{13}\text{C}_{\text{PDB}}$ 值呈负相关, 反映出有机质参与形成了锰碳酸盐, 这也是矿石和围岩 Z 值偏低而不能有效区分海相和湖相碳酸盐沉积的根本原因.

(2) 同位素外部测温法结果显示, 围岩古温度集中分布在 $66.60 \sim 70.40\text{ }^\circ\text{C}$, 矿石古温度为 $57.97 \sim 64.73\text{ }^\circ\text{C}$; 同位素分馏方程模拟计算结果显示, 围岩古温度集中分布在 $59.00 \sim 78.00\text{ }^\circ\text{C}$, 矿石古温度为 $71.00 \sim 92.00\text{ }^\circ\text{C}$. 尽管两种推算结果有一定的差别, 但均证明东平富 Ga 含锰岩系为热水沉积成因.

(3) 东平富 Ga 含锰岩系 Ga 的来源与海底热液活动密切相关. 海底热液活动在成矿过程中起着关键性作用, 一方面直接或间接提供了形成锰碳酸盐所需要的大量有机质; 另一方面带来了大量 Ga, 被锰的氧化物或氢氧化物所吸附, 同时还被海洋生物 (多为热液微生物) 所富集, 而后经复杂的成岩和成矿作用而最终赋存于含锰岩系之中形成富 Ga 含锰岩系.

References

- An, C. B., Feng, Z. D., Barton, L., 2006. Dry or Humid? Mid-Holocene Humidity Changes in Arid and Semi-Arid China. *Quaternary Science Reviews*, 25 (3-4): 351-361. doi:10.1016/j.quascirev.2005.03.013
- Anikeeva, L. I., Kazakova, V. E., Gavrilenko, G. M., 2008. Ferromanganese Crust Formations of the West Pacific Transition Zone. *Vestnik KRAUNTS, Nauki o Zemle*, 11 (1): 10-31 (in Russian with English abstract).
- Baturin, G. N., Dobretsova, I. G., Dubinchuk, V. T., 2014. Hydrothermal Manganese Mineralization in the Peterburgskoye Ore Field (North Atlantic). *Oceanology*, 54 (2): 222-230. doi:10.1134/s0001437014020027
- Baturin, G. N., Dubinchuk, V. T., Rashidov, V. A., 2011. Distribution of Microelements in Ferromanganese Crusts of the Sea of Okhotsk. *Doklady Earth Sciences*, 440 (1): 1291-1297. doi:10.1134/s1028334x11090121

- Baturin, G. N., Dubinchuk, V. T., Rashidov, V. A., 2012. Ferromanganese Crusts from the Sea of Okhotsk. *Oceanology*, 52(1): 88–100. doi: 10.1134/s0001437012010031
- Baturin, G. N., Dubinchuk, V. T., Savels'ev, D. P., et al., 2010. Ferromanganese Crusts on the Bottom of the Bering Sea. *Doklady Earth Sciences*, 435(1): 1478–1482. doi: 10.1134/s1028334x10110152
- Benézeth, P., Diakonov, I. I., Pokrovski, G. S., et al., 1997. Gallium Speciation in Aqueous Solution. Experimental Study and Modelling: Part 2. Solubility of α -GaOOH in Acidic Solutions from 150 to 250 °C and Hydrolysis Constants of Gallium (III) to 300 °C. *Geochimica et Cosmochimica Acta*, 61(7): 1345–1357. doi: 10.1016/s0016-7037(97)00012-4
- Boni, M., Parente, G., Bechstädt, T., et al., 2000. Hydrothermal Dolomites in SW Sardinia (Italy): Evidence for a Widespread Late-Variscan Fluid Flow Event. *Sedimentary Geology*, 131(3–4): 181–200. doi: 10.1016/s0037-0738(99)00131-1
- Chen, J., Wang, H. N., 2004. Geochemistry. Science Press, Beijing (in Chinese).
- Coleman, M., Fleet, A., Donson, P., 1982. Preliminary Studies of Manganese-Rich Carbonate Nodules from Leg 68, Site 503, Eastern Equatorial Pacific. *Initial Reports of the Deep Sea Drilling Project*, 68: 481–489. doi: 10.2973/dsdp.proc.68.123.1982
- Colwell, R. R., 1997. Microbial Diversity: The Importance of Exploration and Conservation. *Journal of Industrial Microbiology and Biotechnology*, 18(5): 302–307. doi: 10.1038/sj.jim.2900390
- Dai, S. F., Ren, D. Y., Chou, C. L., et al., 2012. Geochemistry of Trace Elements in Chinese Coals: A Review of Abundances, Genetic Types, Impacts on Human Health, and Industrial Utilization. *International Journal of Coal Geology*, 94: 3–21. doi: 10.1016/j.coal.2011.02.003
- Derry, L. A., 2010. On the Significance of $\delta^{13}\text{C}$ Correlations in Ancient Sediments. *Earth and Planetary Science Letters*, 296(3–4): 497–501. doi: 10.1016/j.epsl.2010.05.035
- Díaz-del-Río, V., Somoza, L., Martínez-Frias, J., et al., 2003. Vast Fields of Hydrocarbon-Derived Carbonate Chimneys Related to the Accretionary Wedge/Olistostrome of the Gulf of Cádiz. *Marine Geology*, 195(1–4): 177–200. doi: 10.1016/s0025-3227(02)00687-4
- Dubinin, A. V., Uspenskaya, T. Y., 2006. Geochemistry and Specific Features of Manganese Ore Formation in Sediments of Oceanic Bioproductive Zones. *Lithology and Mineral Resources*, 41(1): 1–14. doi: 10.1134/s0024490206010019
- Dubinin, A. V., Uspenskaya, T. Y., Gavrilenko, G. M., et al., 2008. Geochemistry and Genesis of Fe-Mn Mineralization in Island Arcs in the West Pacific Ocean. *Geochemistry International*, 46(12): 1206–1227. doi: 10.1134/s0016702908120021
- Fio, K., Sremac, J., Vlahović, I., et al., 2013. Permian Deposits and the Permian-Triassic Boundary in Croatia: Palaeoclimatic Implications Based on Palaeontological and Geochemical Data. *Geological Society, London, Special Publications*, 376(1): 539–548. doi: 10.1144/sp376.8
- Gao, J. B., Yang, R. D., Tao, P., et al., 2013. Geochemical Characteristics and Genesis of Large Devonian Barite Deposits in Zhenning County, Guizhou Province. *Geoscience*, 27(1): 46–55 (in Chinese with English abstract).
- Ghosh, P., Adkins, J., Affek, H., et al., 2006. ^{13}C - ^{18}O Bonds in Carbonate Minerals: A New Kind of Paleothermometer. *Geochimica et Cosmochimica Acta*, 70(6): 1439–1456. doi: 10.1016/j.gca.2005.11.014
- Glasby, G. P., Stüben, D., Jeschke, G., et al., 1997. A Model for the Formation of Hydrothermal Manganese Crusts from the Pitcairn Island Hotspot. *Geochimica et Cosmochimica Acta*, 61(21): 4583–4597. doi: 10.1016/s0016-7037(97)00262-7
- Han, X. T., Bao, Z. Y., Xie, S. Y., 2016. Origin and Geochemical Characteristics of Dolomites in the Middle Permian Formation, SW Sichuan Basin, China. *Earth Science*, 41(1): 167–176 (in Chinese with English abstract).
- He, Z. W., Yang, R. D., Gao, J. B., et al., 2013. Geological and Geochemical Characteristics of Manganese-Bearing Rock Series of Yangjiawan Manganese Deposit, Songtao County, Guizhou Province. *Geoscience*, 27(3): 593–602 (in Chinese with English abstract).
- Hudson, J. D., 1977. Stable Isotopes and Limestone Lithification. *Journal of the Geological Society*, 133(6): 637–660. doi: 10.1144/gsjgs.133.6.0637
- Iizasa, K., Fiske, R. S., Ishizuka, O., et al., 1999. A Kuroko-Type Polymetallic Sulfide Deposit in a Submarine Silicic Caldera. *Science*, 283(5404): 975–977. doi: 10.1126/science.283.5404.975
- Jia, Y. Y., Xing, X. J., Sun, G. Q., et al., 2015. The Paleogene-Neogene Paleoclimate Evolution in Western Sector of Northern Margin of Qaidam Basin. *Earth Science*, 40(12): 1955–1967 (in Chinese with English abstract).
- Kazachenko, V. T., Miroshnichenko, N. V., Perevoznikova, E. V., et al., 2006. Gallium, Gold, and Platinum Group Metals in Manganese Rocks of Southern Sikhote Alin. *Doklady Earth Sciences*, 407(2): 429–433. doi: 10.1134/s1028334x06030184

- Keith, M. L., Weber, J. N., 1964. Carbon and Oxygen Isotopic Composition of Selected Limestones and Fossils. *Geochimica et Cosmochimica Acta*, 28(10-11): 1787-1816. doi: 10.1016/0016-7037(64)90022-5
- Koschinsky, A., Hein, J. R., 2003. Uptake of Elements from Seawater by Ferromanganese Crusts; Solid-Phase Associations and Seawater Speciation. *Marine Geology*, 198(3-4): 331-351. doi: 10.1016/s0025-3227(03)00122-1
- Kuleshov, V. N., 2011. Manganese Deposits; Communication 1. Genetic Models of Manganese Ore Formation. *Lithology and Mineral Resources*, 46(5): 473-493. doi: 10.1134/s0024490211050038
- Kuleshov, V. N., Brusnitsyn, A. I., 2005. Isotopic Composition ($\delta^{13}\text{C}$, $\delta^{18}\text{O}$) and the Origin of Carbonates from Manganese Deposits of the Southern Urals. *Lithology and Mineral Resources*, 40(4): 364-375. doi: 10.1007/s10987-005-0034-8
- Li, D., Ling, H. F., Jiang, S. Y., et al., 2009. New Carbon Isotope Stratigraphy of the Ediacaran-Cambrian Boundary Interval from SW China: Implications for Global Correlation. *Geological Magazine*, 146(4): 465. doi: 10.1017/s0016756809006268
- Li, S. F., Wang, Z. H., Li, L. T., et al., 2009. Analysis of Metallogenic Mechanism of High-Grade Manganese Ore in Southwest Guangxi. *Resources Environment & Engineering*, 23(4): 363-370 (in Chinese with English abstract).
- Li, X. Z., Liu, W. G., Xu, L. M., 2012. Carbon Isotopes in Surface-Sediment Carbonates of Modern Lake Qinghai (Qinghai-Tibet Plateau): Implications for Lake Evolution in Arid Areas. *Chemical Geology*, 300-301: 88-96. doi: 10.1016/j.chemgeo.2012.01.010
- Liu, T. F., 1996. Study on Geological Feature and Metallogenic Conditions of Dongping Supergene Enriched Mn Ore Deposit. *Contributions to Geology and Mineral Resources Research*, 11(4): 42-55 (in Chinese with English abstract).
- Liu, Y. J., Cao, L. M., Li, Z. L., et al., 1984. Element Geochemistry. Science Press, Beijing (in Chinese).
- Liu, Z. C., Zhang, Y. G., Chen, D., et al., 2013. Geochemical Characteristics and Geological Significance of "Bainitangceng" Siliceous Rocks in Zunyi Manganese Ore Fields, Guizhou Province, China. *Acta Mineralogica Sinica*, 33(4): 665-670 (in Chinese with English abstract).
- Lloyd, S. J., Corsetti, F. A., Eagle, R. A., et al., 2015. Evolution of Neoproterozoic Wonoka-Shuram Anomaly-Aged Carbonates: Evidence from Clumped Isotope Paleothermometry. *Precambrian Research*, 264: 179-191. doi: 10.1016/j.precamres.2015.04.010
- Macouin, M., Ader, M., Moreau, M. G., et al., 2012. Deciphering the Impact of Diagenesis Overprint on Negative $\delta^{13}\text{C}$ Excursions Using Rock Magnetism: Case Study of Ediacaran Carbonates, Yangjiaping Section, South China. *Earth and Planetary Science Letters*, 351-352: 281-294. doi: 10.1016/j.epsl.2012.06.057
- Metz, S., Trefry, J. H., 2000. Chemical and Mineralogical Influences on Concentrations of Trace Metals in Hydrothermal Fluids. *Geochimica et Cosmochimica Acta*, 64(13): 2267-2279. doi: 10.1016/s0016-7037(00)00354-9
- Mikhailik, P. E., Derkachev, A. N., Chudaev, O. V., et al., 2009. Fe-Mn Crusts from Underwater Rises of the Kasehevarov Trough (Sea of Okhotsk). *Russian Journal of Pacific Geology*, 3(1): 28-39. doi: 10.1134/s1819714009010047
- Mikhailik, P. E., Khanchuk, A. I., 2011. Ferromanganese Crusts from Submarine Volcanoes of Backarc Basins as a New Genetic Type of Gallium Deposits. *Doklady Earth Sciences*, 439(2): 1060-1062. doi: 10.1134/s1028334x11080058
- Mikhailik, P. E., Mikhailik, E. V., Blokhin, M. G., et al., 2015. Sources of Gallium in Ferromanganese Crusts from the Sea of Japan. *Russian Geology and Geophysics*, 56(8): 1148-1153. doi: 10.1016/j.rgg.2015.07.005
- Mishra, P., Mvohapatra, B. K., Singh, P. P., 2006. Mode of Occurrence and Characteristics of Mn-Ore Bodies in Iron Ore Group of Rocks, North Orissa, India and Its Significance in Resource Evaluation. *Resource Geology*, 56(1): 55-64. doi: 10.1111/j.1751-3928.2006.tb00268.x
- Moskalyk, R. R., 2003. Gallium: The Backbone of the Electronics Industry. *Minerals Engineering*, 16(10): 921-929. doi: 10.1016/j.mineng.2003.08.003
- Noguchi, T., Oomori, T., Tanahara, A., et al., 2007. Chemical Composition of Hydrothermal Ores from Mid-Okinawa Trough and Suiyo Seamount Determined by Neutron Activation Analysis. *Geochemical Journal*, 41(2): 141-148. doi: 10.2343/geochemj.41.141
- Okita, P. M., Maynard, J. B., Spiker, E. C., et al., 1988. Isotopic Evidence for Organic Matter Oxidation by Manganese Reduction in the Formation of Stratiform Manganese Carbonate Ore. *Geochimica et Cosmochimica Acta*, 52(11): 2679-2685. doi: 10.1016/0016-7037(88)90036-1
- Okita, P. M., Shanks, W. C., 1992. Origin of Stratiform Sediment-Hosted Manganese Carbonate Ore Deposits: Examples from Molango, Mexico, and Taojiang, China. *Chemical Geology*, 99(1-3): 139-163. doi: 10.1016/0009-2541(92)90036-5
- O'Neil, J. R., Epstein, S., 1966. Oxygen Isotope Fractionation

- in the System Dolomite-Calcite-Carbon Dioxide. *Science*, 152 (3719): 198—201. doi: 10.1126/science.152.3719.198
- Papp, D.C., Cociuba, I., Lazăr, D.F., 2013. Carbon and Oxygen-Isotope Stratigraphy of the Early Cretaceous Carbonate Platform of Pădurea Craiului (Apuseni Mountains, Romania): A Chemostratigraphic Correlation and Paleoenvironmental Tool. *Applied Geochemistry*, 32: 3—16. doi: 10.1016/j.apgeochem.2012.09.005
- Ru, T.Q., Wei, L.D., Shu, G., 1992. Geological Characteristics of Manganese Ores in Guangxi. Geological Publishing House, Nanjing (in Chinese).
- Saalen, G., Doyle, P., Talbot, M.R., 1996. Stable-Isotope Analyses of Belemnite Rostra from the Whitby Mudstone Fm., England; Surface Water Conditions during Deposition of a Marine Black Shale. *Palaios*, 11(2): 97. doi: 10.2307/3515065
- Shackleton, N.J., Kennett, J.P., 1975. Paleotemperature History of the Cenozoic and the Initiation of Antarctic Glaciation: Oxygen and Carbon Isotope Analyses in DSDP Sites 277, 279 and 281. *Initial Reports of the Deep Sea Drilling Project*, 29: 743—755. doi: 10.2973/dsdp.proc.29.117.1975
- Shao, J. N., Tao, W. P., 2010. Mineral Resources Industry Handbook. Geological Publishing House, Beijing (in Chinese).
- Sugisaki, R., Sugitani, K., Adachi, M., 1991. Manganese Carbonate Bands as an Indicator of Hemipelagic Sedimentary Environments. *The Journal of Geology*, 99 (1): 23—40. doi: 10.1086/629471
- Sverdrup, H. U., Ragnarsdóttir, K. V., 2014. Section 2. Classification of Natural Resources. *Geochemical Perspectives*, 3(2): 172—192.
- Telford, M., 2001. Gallium Shortage Easing. *III-Vs Review*, 14(4): 54—58. doi: 10.1016/s0961-1290(01)80184-8
- Wang, H. W., Wen, X. P., Chang, H. L., et al., 2013. Characteristics of Carbon and Oxygen Isotope in Heqing Manganese Deposit, Yunnan, China. *Geoscience*, 27(3): 612—620 (in Chinese with English abstract).
- Wefer, G., Berger, W. H., 1991. Isotope Paleontology: Growth and Composition of Extant Calcareous Species. *Marine Geology*, 100 (1—4): 207—248. doi: 10.1016/0025-3227(91)90234-u
- Yang, K. H., Yu, X. G., Chu, F. Y., et al., 2016. Environmental Changes in Methane Seeps Recorded by Carbon and Oxygen Isotopes in the Northern South China Sea. *Earth Science*, 41 (7): 1206—1215 (in Chinese with English abstract).
- Yang, R. D., Cheng, M. L., Wei, H. R., 2009. Geochemical Characteristics and Origin of a Manganese Deposit in the Middle Permian Maokou Formation in Shuicheng, Guizhou, China. *Geotectonica et Metallogenia*, 33 (4): 613—619 (in Chinese with English abstract).
- Yang, R. D., Gao, J. B., Cheng, M. L., et al., 2010. Sedimentary Geochemistry of Manganese Deposit of the Neoproterozoic Datangpo Formation in Guizhou Province, China. *Acta Geologica Sinica*, 84(12): 1781—1790 (in Chinese with English abstract).
- Yang, X. F., Liu, C., Chen, X., 2013. Discussion on Ore Characteristics and Ore-Forming Mechanism of Baishixi Manganese Deposit, Guizhou. *Geotechnical Engineering World*, 4 (1): 52—55 (in Chinese with English abstract).
- Yang, Y., Gao, F. H., Pu, X. G., et al., 2013. Changes to Depositional Palaeoenvironments within the Qikou Depression (Bohaiwan Basin, China): Carbon and Oxygen Isotopes in Lacustrine Carbonates of the Palaeogene Shahejie Formation. *International Geology Review*, 55 (15): 1909—1921. doi: 10.1080/00206814.2013.805926
- Yi, F., Yi, H. S., 2017. Geochemical Characteristics of the Beisi Formation Manganese-Bearing Rocks of the Lower Triassic Series in the Tiandeng Area, Southwest Guangxi and Their Implications. *Geochimica*, 46 (1): 46—65 (in Chinese with English abstract).
- Yi, H. S., Chen, Z. Y., Ji, C. J., et al., 2014. New Evidence for Deep Burial Origin of Sucrosic Dolomites from Middle Jurassic Buqu Formation in Southern Qiangtang Basin. *Acta Petrologica Sinica*, 30(3): 737—746 (in Chinese with English abstract).
- Yin, Q., 2015. Research on Depositional Feature and Mineralization Mechanism of Manganese Deposit of the Lower Triassic in Southwestern Guangxi Area (Dissertation). Chengdu University of Technology, Chengdu (in Chinese with English abstract).
- Zeng, Z. G., 2011. Seafloor Hydrothermal Geology. Science Press, Beijing (in Chinese).
- Zhang, C., 2013. Sedimentation Feature of Manganese-Bearing Rock Series from the Upper Devonian, Southwest of Guangxi, China (Dissertation). Chengdu University of Technology, Chengdu (in Chinese with English abstract).
- Zhang, Z. W., Ding, H. S., Zhang, Y. J., 2016. Carbon and Oxygen Stable Isotope Features of the Lower Ordovician Gucheng Region of Tarim Basin. *Marine Geology & Quaternary Geology*, 36 (2): 59—64 (in Chinese with English abstract).
- Zheng, Y. F., 1999. Oxygen Isotope Fractionation in Carbonate and Sulfate Minerals. *Geochemical Journal*, 33(2):

109–126. doi:10.2343/geochemj.33.109

Zhu, S. Q., 1997. Geochemical Characteristics of Rare Earth Elements in Dongping Manganese Deposit, Guangxi. *South China Metallurgical Geology*, 2: 27–30 (in Chinese).

Zhu, S. Q., 2001. Phodochrosite of Hemioxidative Zone in Dongping Manganese Ore. *Geology and Prospecting*, 37 (2): 58–61 (in Chinese with English abstract).

Zuo, J. X., Tong, J. N., Qiu, H. O., et al., 2006. Carbon Isotope Composition of the Lower Triassic Marine Carbonates, Lower Yangtze Region, South China. *Science China Earth Science*, 49(3): 225–241. doi:10.1007/s11430-006-0225-8

附中文参考文献

陈骏, 王鹤年, 2004. 地球化学. 北京: 科学出版社.

高军波, 杨瑞东, 陶平, 等, 2013. 贵州镇宁泥盆系大型重晶石矿床地球化学特征及其成因研究. *现代地质*, 27(1): 46–55.

韩晓涛, 鲍征宇, 谢淑云, 2016. 四川盆地西南中二叠统白云岩的地球化学特征及其成因. *地球科学*, 41(1): 167–176.

何志威, 杨瑞东, 高军波, 等, 2013. 贵州省松桃杨家湾锰矿含锰岩系地质地球化学特征. *现代地质*, 27(3): 593–602.

贾艳艳, 邢学军, 孙国强, 等, 2015. 柴北缘西段古—新近纪古气候演化. *地球科学*, 40(12): 1955–1967.

李升福, 王泽华, 李朗田, 等, 2009. 桂西南优质锰矿成矿机理分析. *资源环境与工程*, 23(4): 363–370.

刘腾飞, 1996. 广西东平表生富集型锰矿床地质特征及成矿条件初步研究. *地质找矿论丛*, 11(4): 42–55.

刘英俊, 1984. 元素地球化学. 北京: 科学出版社.

刘志臣, 张远国, 陈登, 等, 2013. 贵州遵义锰矿区“白泥塘层”硅质岩地球化学特征及其地质意义. *矿物学报*, 33(4): 665–670.

茹廷镛, 1992. 广西锰矿地质. 南京: 地质出版社.

邵厥年, 陶维屏, 2010. 矿产资源工业要求手册. 北京: 地质出版社.

王宏伟, 温兴平, 常海亮, 等, 2013. 云南鹤庆锰矿碳氧同位素特征分析. *现代地质*, 27(3): 612–620.

杨克红, 于晓果, 初凤友, 等, 2016. 南海北部甲烷渗漏系统环境变化的碳、氧同位素记录. *地球科学*, 41(7): 1206–1215.

杨瑞东, 程玛莉, 魏怀瑞, 2009. 贵州水城二叠系茅口组含锰岩系地质地球化学特征与锰矿成因分析. *大地构造与成矿学*, 33(4): 613–619.

杨瑞东, 高军波, 程玛莉, 等, 2010. 贵州从江高增新元古代大塘坡组锰矿沉积地球化学特征. *地质学报*, 84(12): 1781–1790.

杨晓飞, 刘畅, 陈旭, 2013. 贵州白石溪锰矿矿石特征及成矿机制探讨. *矿产勘查*, 4(1): 52–55.

伊帆, 伊海生, 2017. 桂西南地区下三叠统北泗组含锰岩系地球化学特征及意义. *地球化学*, 46(1): 46–65.

伊海生, 陈志勇, 季长军, 等, 2014. 羌塘盆地南部地区布曲组砂糖状白云岩埋藏成因的新证据. *岩石学报*, 30(3): 737–746.

尹青, 2015. 桂西南地区下三叠统锰矿沉积特征与成因机理研究(博士学位论文). 成都: 成都理工大学.

曾志刚, 2011. 海底热液地质学. 北京: 科学出版社.

张超, 2013. 桂西南地区上泥盆统含锰岩系沉积特征研究(硕士学位论文). 成都: 成都理工大学.

张振伟, 丁寒生, 张亚金, 2016. 塔里木盆地古城地区下奥陶统碳酸盐岩碳氧同位素特征. *海洋地质与第四纪地质*, 36(2): 59–64.

祝寿泉, 1997. 广西东平锰矿稀土元素地球化学特征. *中南冶金地质*, (2): 27–30.

祝寿泉, 2001. 广西东平锰矿半氧化带中的菱锰矿. *地质与勘探*, 37(2): 58–61.